2D-EULER DECONVOLUTION AND FORWARD MODELING OF GRAVITY DATA OF HOMA-HILLS GEOTHERMAL PROSPECT, KENYA

A. Odek[1], A. B. Otieno[1], W. J. Ambusso[1] and J. G. Githiri[2]
[1] Kenyatta University, Nairobi
[2] Jomo Kenyatta University of Agriculture and Technology, Nairobi
E-mail: odekantony@yahoo.com

Abstract
In order to fully assess the potential of Homa Hills Geothermal prospect, the heat source which is one of the main features of a geothermal system had to be located based on its perturbation on the gravity field. Ground gravity survey was conducted in an area covering about 76 km2 and the data processed to remove all other effects which are not of geological interest. Qualitative interpretation was attempted and cross sections drawn across the anomalous areas on the complete Bouguer anomaly map. Quantitative interpretation attempted involved both Euler Deconvolution and 2-D Forward modelling. The parameters obtained from Euler Deconvolution were used as the start up parameters for 2-D Forward modeling. Well clustered Euler solutions were obtained at a shallow depth of approximately 200-750 m which is consistent with the modeled shallow dike like intrusive probably of carbonatite origin.

Key words: gravity, anomalies, Homa Hills, heat source, Euler-Deconvolution

1.0 Introduction

The manifestation of hot springs and steaming grounds in Homa-Hills has revealed its geothermal potential. Earlier research conducted using Magnetotelluric (MT) and Transient Electromagnetics (TEM) by Geothermal Development Company revealed a relatively deep seated heat source characterized by shallow dikes. Gravity technique which is a high precision method for measuring density contrast that relates to the subsurface rocks was conducted as a follow-up technique. The variation of density in a geothermal environment is as a result of magma intruding the crust informs of dikes, sills and other structural conditions of the subsurface rocks. In order to locate the intruding structures gravity data was collected from 87 stations established over an area of 76 km2 bounded by the latitudes 34.547˚E - 34.473˚E and longitudes 0.4276˚S – 0.3344˚S in Homa Hills geothermal prospect, with both station and profile spacing of 500 m. Relative gravity measurements were taken using Worden gravity meter model prospector 410. All the gravity corrections were made for the effects which are not of direct geological interest, which includes correction for instrumental drift, free air, latitude, Bouger slab and terrain, the complete Bouger anomaly should contain information about the subsurface density alone. A contour map of the Bouger anomaly Figure 1 gives a good impression of subsurface density. The interpretation of gravity data involved identifying the anomalies from the Bouger anomaly map, selecting profiles across the anomalies as shown in Figure 1 and subjecting the profiles to both Euler deconvolution and Forward modeling.

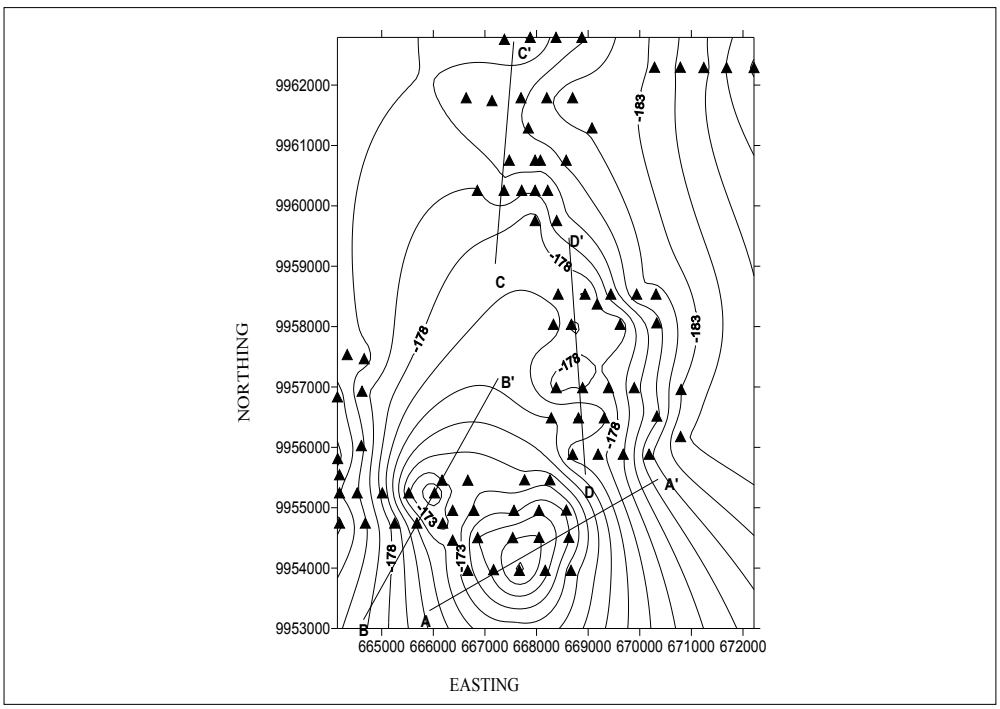

Figure 1: Complete Bouguer anomaly contour map

1.1 Study Area

Homa Hills geothermal field is located in the Nyanzian rift west of Kendu, a branch of East African rift valley which occupies most of the Homa peninsula and protrudes into the Kavirondo Gulf. The Kenyan part of East African Rift is oriented in the N-S trending with crustal thickness of 20 km in the North and 35 km at the centre and forms an active continental extension with a length of about 500 km, a width of 60-80 km and an average cross-sectional relieve of more than 1000 m. It is characterized by intense faulting, seismic activity and abnormally high heat flow (Baker and Wohlenberg, 1971). The northern, central and southern segment of the Kenyan Rift have half graben geometries due to earlier faulting and pronounced subsidence along the western boundary faults. The N80°E trending Nyanza half-graben branches with the main Kenyan rift at Menengai where there is a triple junction and disappears westward under Lake Victoria (Figure 2).

1.2 Geological and Tectonic Setting

Homa Mountain is a site of an active volcano in tertiary and Pleistocene times. It is composed of a number of massive separate peaks which include Homa, Nyasanja and Apoyo. The largest (Homa) rises to a height of over 5200 ft. The mountain is cloaked to its lower slopes by thick mantle of pleistoscene and recent sediments. The country rocks to the south and towards north of the mountain are composed of rhyolitic, andesitic and basaltic Nyanzian lavas which have been highly folded and form an anticlinorium pitching south-westwards (Figure 3). These rocks are mildly metamorphosed and have been invaded by carbonatitic dikes of various types. There are no rocks representing the Paleozoic and Mesozoic eras, but intrusive, tectonic, volcanic and depositional activity occurred in the tertiary era. The location of the mountain is a weakened.

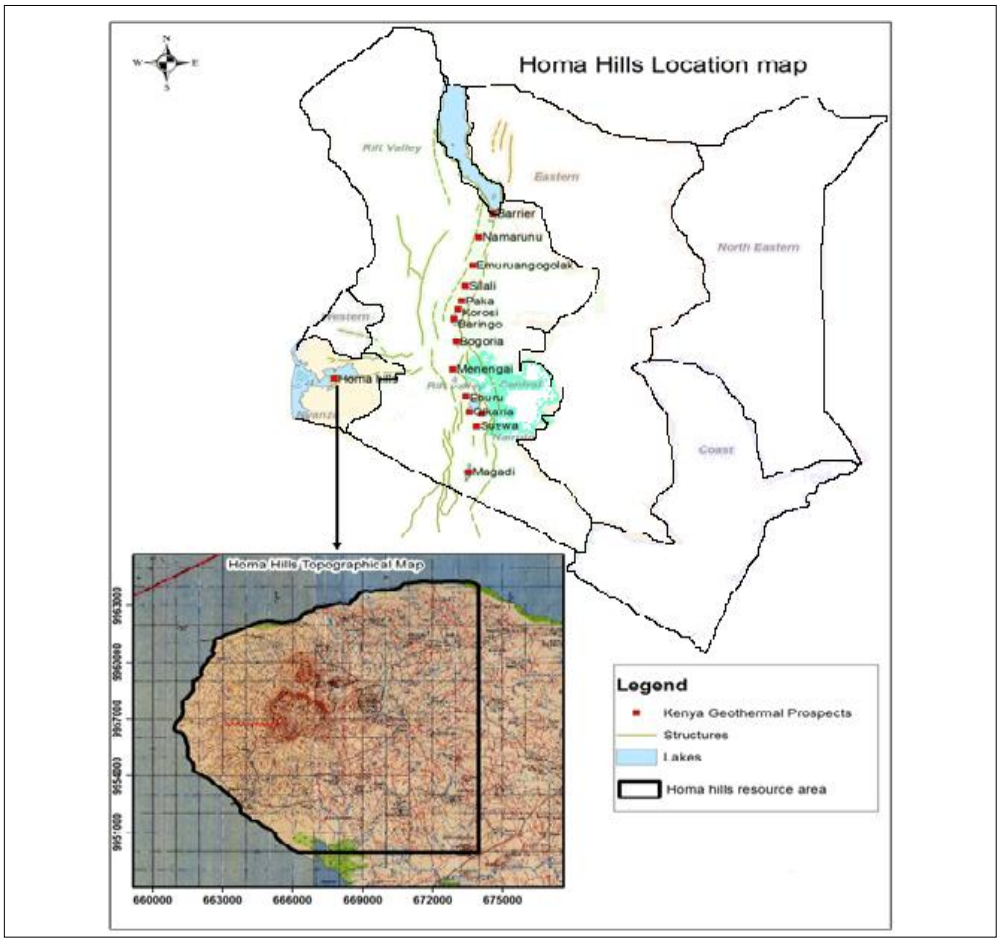

Figure 2: Location of Homa-Hills geothermal prospect

zone near the intersection of Kendu fault to the north and Samanga fault to the south east of the mountain. Nyanzian rift is responsible for the formation of Homa Mountain and Crater Lake Simbi (Saggerson, 1952).

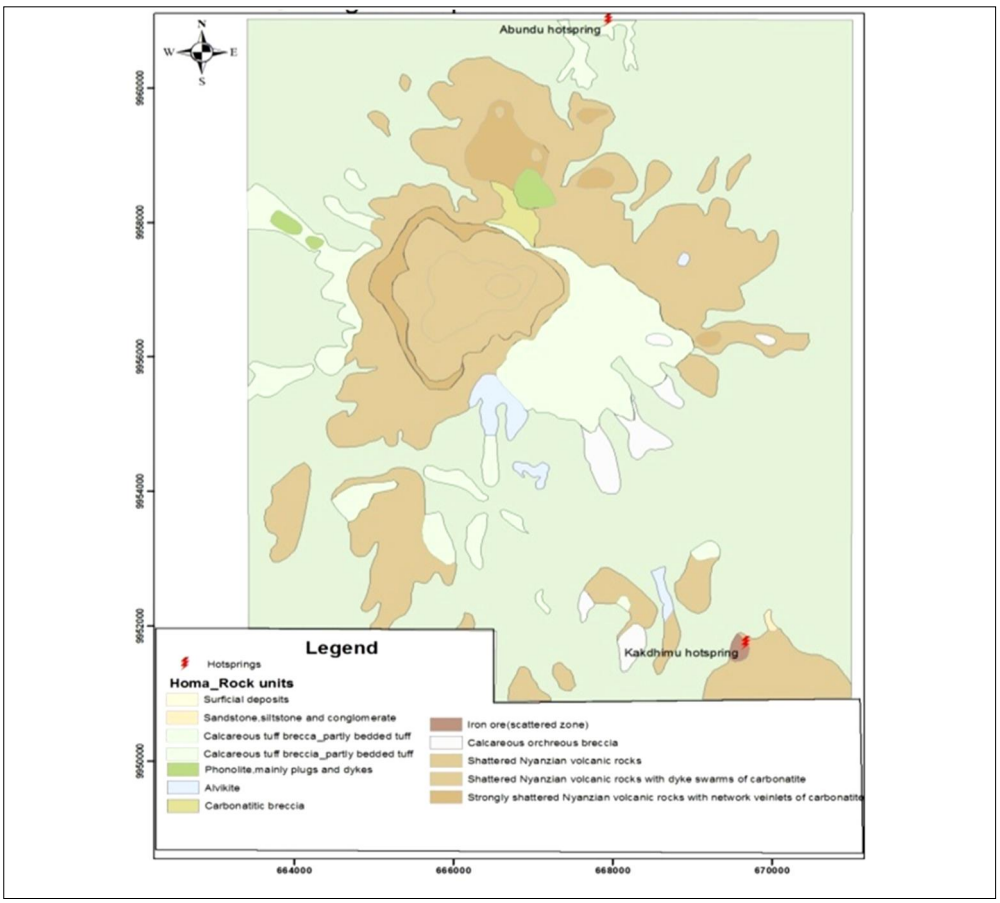

Figure 3: Geologic map of Homa Hills geothermal prospect

4.0 Euler deconvolution

4.1 Theory

Euler Deconvolution aids the interpretation of gravity field. It involves determination of the position of the causative body based on an analysis of the gravity field and the gradients of that field and some constraint on the geometry of the body Zhang et al. (2000). The quality of the depth estimation depends mostly on the choice of the proper structural index which is a function of the geometry of the causative bodies and adequate sampling of the data Williams *et al.* (2005). It is based on the Euler equation of homogeneity,

$$(x - x_o)T_{zx} + (y - y_o)T_{zy} + (z - z_o)T_{zz} = n(B_z - T_z) \quad \text{.....1}$$

for the gravity anomaly vertical component Tz of a body having a homogeneous gravity field, (xo, yo, zo) are the unknown co-ordinates of the source body centre to

be estimated. (x, y, z) are the known co-ordinates of the observation points of the gravity and gradients. The values Tzx, Tzy, Tzz are the measured gradients along the x-,y- and z-directions, n is the structural index and Bz is the regional value of the gravity to be estimated. In 2-D this equation reduces to;

$$(x-x_o)T_{zx}+(z-z_o)T_{zz}=n(B_z-T_z) \quad \text{.....} \quad 2$$

There are three unknown parameters (xo,zo and Bz). In this study, a structural index of 0.5 was adopted since it gives the most accurate depth estimates for gravity data where the typical source structures are finite-offset (Williams *et al.,* 2005).

4.2 Interpretation of Euler Solutions

In this study the results were generated using Euler 1.0 software after Cooper (2004). Figures 4(a) and 4(b) below and 4(c) and 4(d) in the appendix shows the vertical and horizontal gradients of the gravity field and 2-D Euler solutions for profiles AA', BB', CC' and DD'. The solutions cluster well at a shallow depth estimated to be between 200 m to 750 m. The depth of these high gravity causative bodies under profiles AA', BB' and DD' coincide well with the geology of the study area which reveals a swarm of shallow dykes of possibly carbonatite nature. Euler deconvolution also captures a less dense structure along profile CC' taken along the shore of Lake Victoria. The less dense alluvial deposit occurs to a depth of approximately 650 m beneath the ground surface over an estimated width of 2000 m (Figure 4(c)). The scattered solutions which are not well constrained (spurious) were rejected during the interpretation.

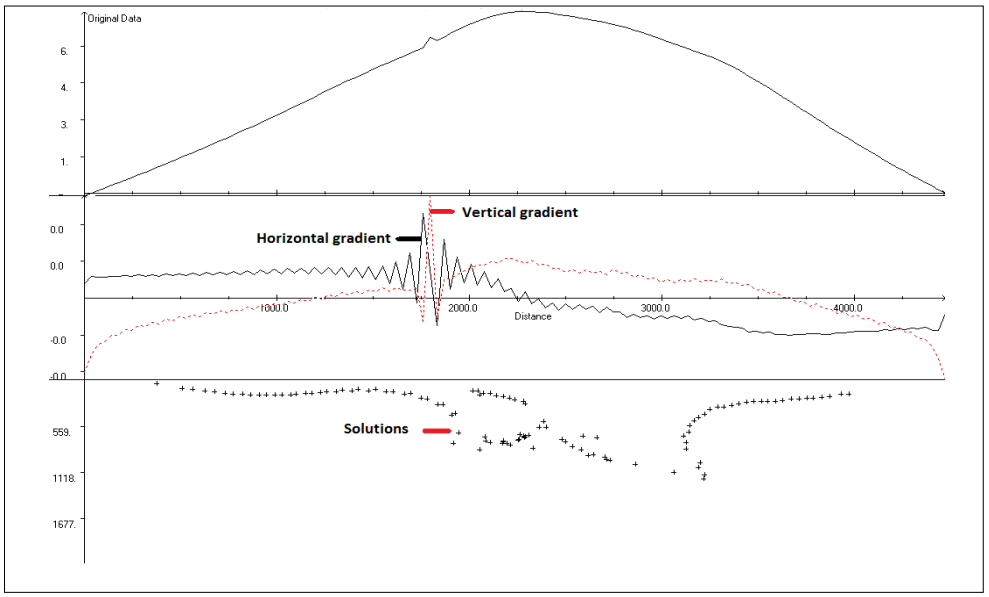

***F**igure 4(a): Euler Deconvolution along profile AA'.*

Conventional Euler deconvolution produces spray of solutions, within which the correct answer for each discrete body needs to be found. Weighted least squares minimize the errors in the solution for best fit and also give local error estimates. In order to distinguish more reliable solutions from spurious ones, some of the discrimination techniques proposed by Desmond et al. (2004) were used, these includes; analysis of the clustering of solutions, rejection of bodies that have inadmissible structural index, low pass filtering of the data to constrain the frequency content and rejection of solutions based on reliability.

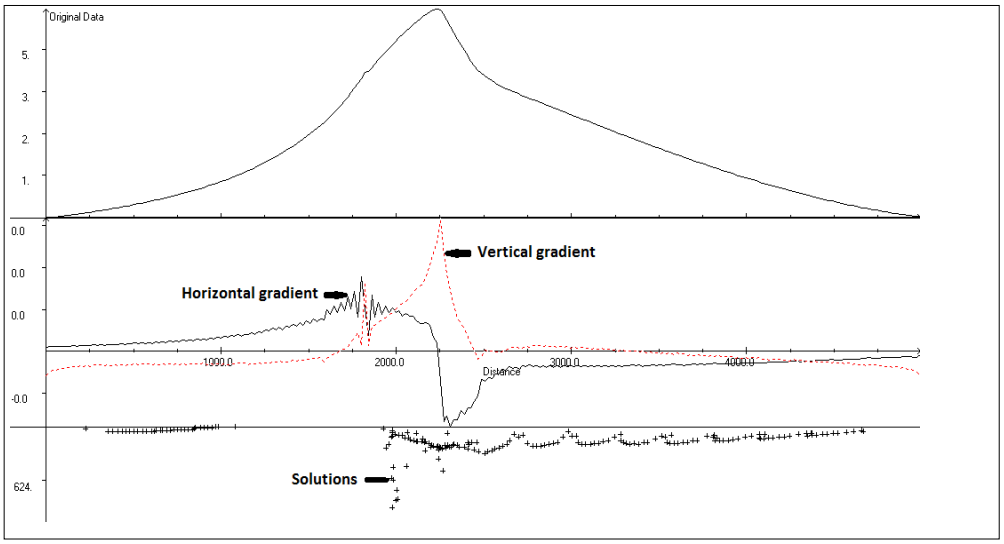

Figure 4(b): Euler Deconvolution along profile BB'

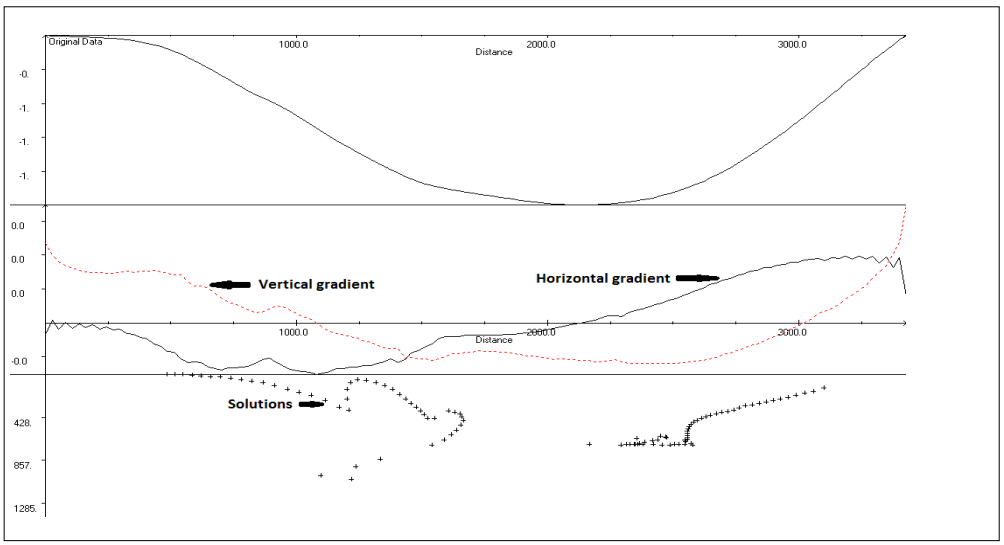

Figure 4(c): Euler Deconvolution along profile CC'.

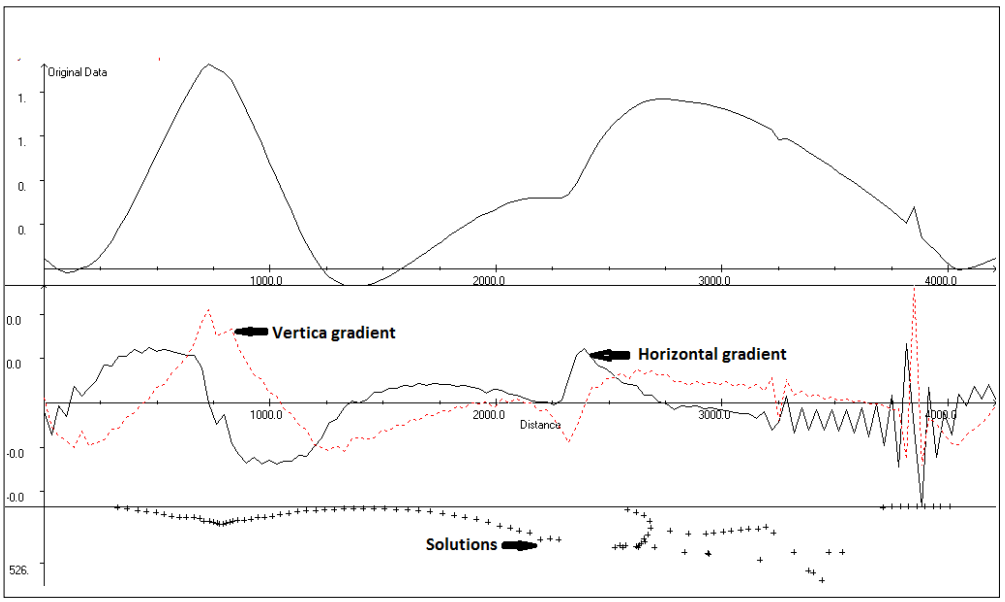

5.0 Forward Modelling

5.1 Theory

Where the shapes and depths of anomaly sources are important, gravity data are usually interpreted by the method of forward modeling, in which the gravity field of a subsurface model prepared using all available geological information, is compared with the field actually observed (Parasnis, 1986). The model is then modified, within the limits set by the geological constraints, until a satisfactory level of agreement is reached between calculation and observation. This process was done using the grav2DC software developed by Talwani et al (1964). The final model is not, of course, necessarily correct, and since other mass distributions will exist that satisfy all the conditions, but it is at least a possible solution. In this study the modifications to the model was performed interactively on a computer screen which shows both the model and the gravity data. Two-dimensional approximations were used in which the geology is assumed not to vary at right angles to the line of profile and section and is generally adequate provided that the strike length of the anomaly is at least three times as great as the cross-strike width (Barker and Wohlenberg, 1971). The start up model depth was obtained from the direct interpretation and Euler deconvolution solutions.

5.2 2-D Forward modelling Interpretations

Profile AA' is used to model the gravity high anomaly centered at grid co-ordinates (668000, 9954500). The result of the forward modeling shows a dome like structure with the maximum depth to the top as 192 m, density contrast 0.2436 g/cm^3 and a width of 3.321 km. Figure 5(a) shows the fit between the computed gravity anomaly curve and the observed anomaly along profile AA'.

Similarly, Profiles BB' is used to model gravity high anomaly centered at grid co-ordinates (666000, 9955200). The best fit is obtained at a depth of about 250 m, density contrast 0.3908g/cm^3 and a width of 604 m. Profile CC' cuts across a gravity low anomaly centered at grid co-ordinates (667800, 9961000) oriented E-W. The modeled structure is a less dense body of density contrast -0.8850 g/cm^3 to a depth of approximately 540 m and a width of 2.674 km. Figure 5(c) displays the fit between the anomaly curve as a result of the calculated body and the observed anomaly curve. The structure possibly represents a sedimentary basin filled with low density unconsolidated sediments. Figure 5 (d) is modeled to be consisting of multiple shallow dike structures of density contrast 0.1035 g/cm^3 sandwiched by less dense structures of density contrast -0.534 g/cm^3.

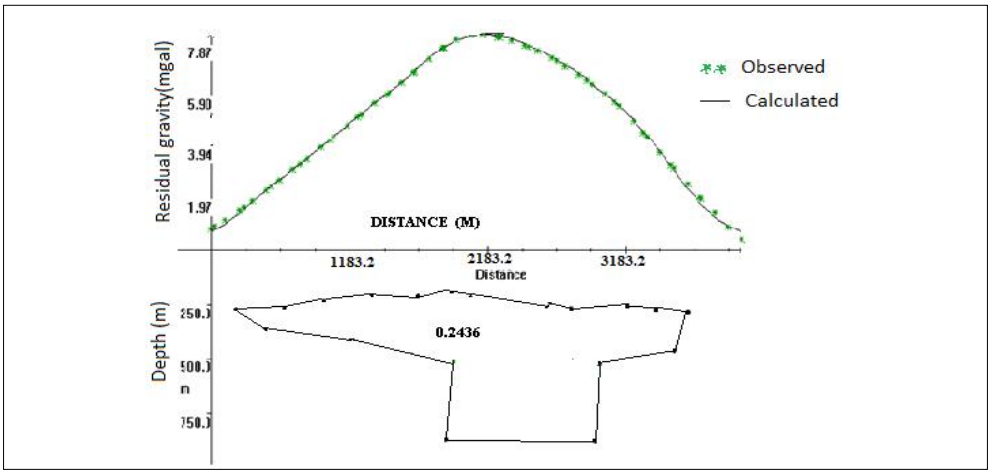

Figure 5(a): Observed, calculated anomaly and forward model for 2-D body along profile AA'.

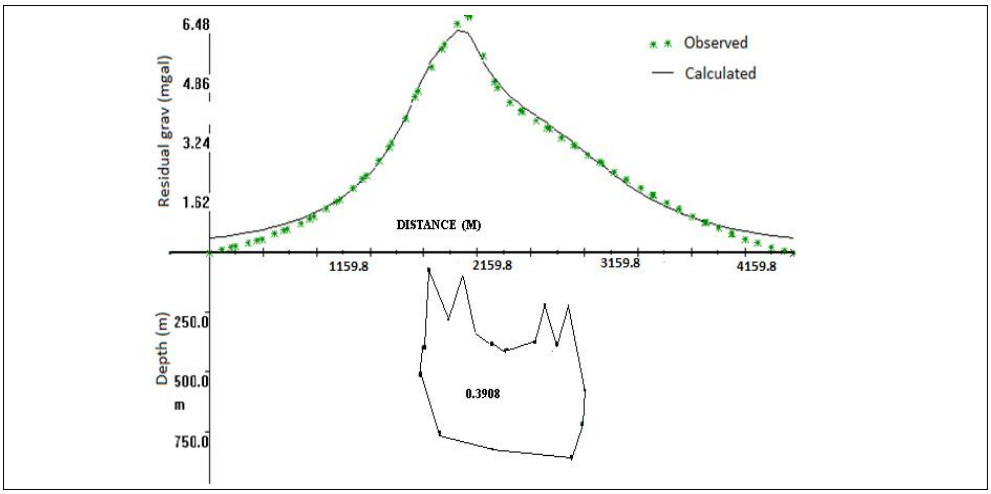

Figure 5(b): Observed, calculated anomaly and forward model for 2-D body along profile BB'.

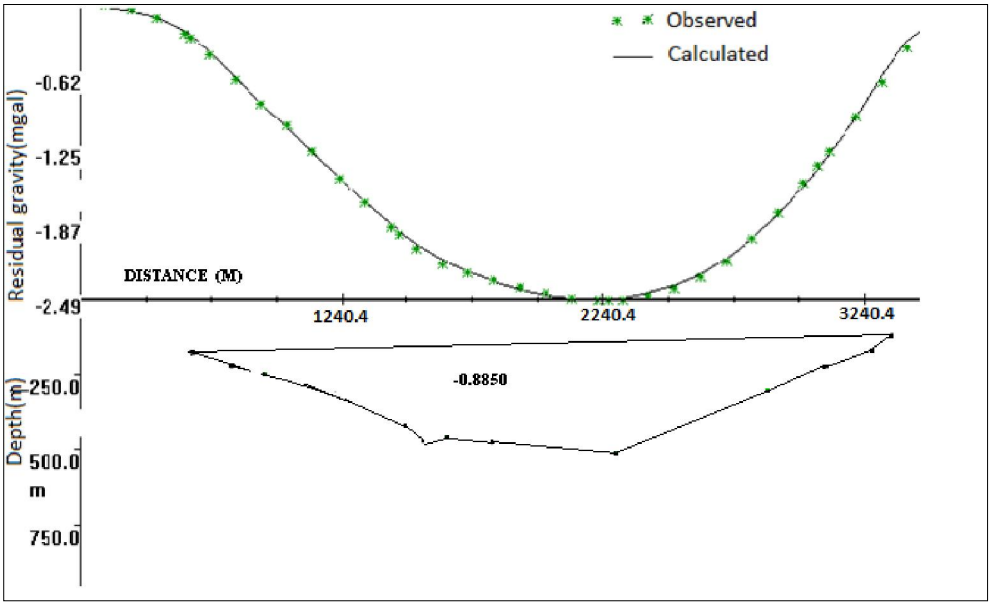

Figure 5(c): Observed, calculated anomaly and forward model for 2-D body along profile CC'.

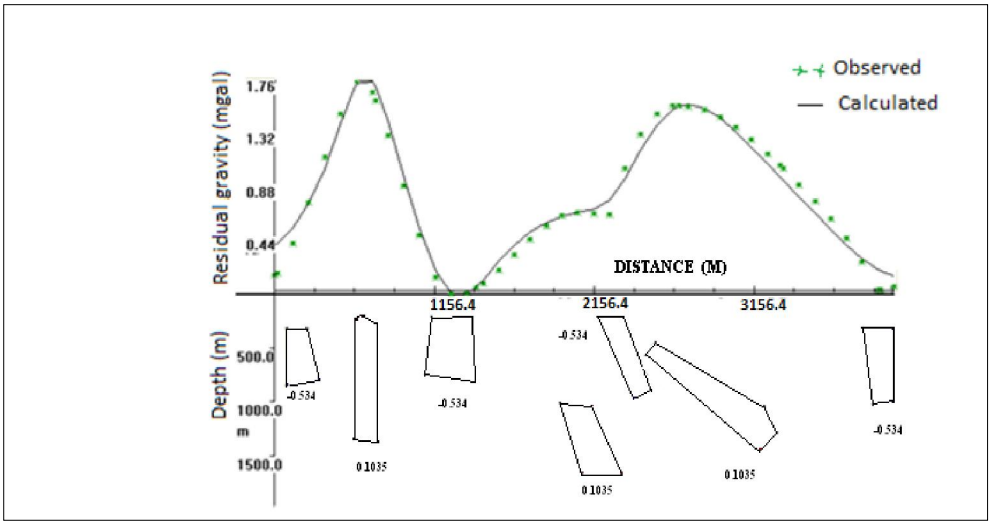

Figure 5(d): Observed, calculated anomaly and forward model for 2-D body along profile DD'.

6.0 Conclusion

The results of this study shows that Homa Hills area has geothermal potential, this supported by presence of the mapped intrusive dikes and high thermal gradient which is manifested through hot springs and steaming ground. The probable heat source is characterized by shallow sharp dikes probably carbonatite in nature which have been modeled to be at a depth of about 200-750 m from the surface on the southern part of the study area.

Acknowledgement

We wish to acknowledge Kenyatta University, Physics department for availing the geophysical survey instruments. We also acknowledge the department of Mines and Geology for availing the geological report of Homa Hills.

References

Baker, B.H. and Wohlenberg, J. (1971). "Structure and evolution of the Kenyan Rift Valley." Nature, 229, 538-542.

Cooper, G.R.J. (2004). "Euler deconvolution applied to potential field gradients." Exploration Geophysics, 35, 165-170.

Desmond, F.G. Philip, M. and Alan R. (2004) "New discrimination techniques for Euler deconvolution". Reid Geophysics, University of Leeds, UK. Computers and Geosciences 30 461-469.

Parasnis D.S. (1986) Principles of Applied Geophysics. Chapman and Hall, U.S.A. 61-103

Saggerson, E.P. (1952). "Geology of the Kisumu District." Degree sheet 41, N.E quadrant. Rep. Geol. Surv. Kenya, 21, 86.

Talwani, M. and Heirtzler, J.R. (1964). "Computation of magnetic anomalies caused by two dimensional structures of arbitrary shape, in Computers in the mineral industries," part 1: Stanford University publications, Geol. Sciences, 9: 464-480.

Williams S.E., Fairhead J.D., and Flanagan G. (2005). "Comparison of grid Euler deconvolution with and without 2D constraints using a realistic 3D magnetic basement model." Geophysics, 70, 13-21.

Zhang C., Mushayandebvu M.F., Reid A.B., Fairhead J.D. and Odegard M.E. (2000). "Euler deconvolution of gravity tensor gradient data." Geophysics, 65, 512-520.